ChemComm

COMMUNICATION

View Article Online
View Journal | View Issue

Cite this: *Chem. Commun.*, 2026, **62**, 4583

Received 26th September 2025,
Accepted 28th January 2026

DOI: 10.1039/d5cc05557a

rsc.li/chemcomm

From solution to thin films: unravelling excited-state behaviour in halogenated diradicaloids

Matteo Bevilacqua,[a] Luca Ciuffarin,[b] Roberto Costantini,[bc] Luca Schio,[c] Albano Cossaro,[dc] Pasquale Orgiani,[c] Federico Cilento,[e] Claudia Graiff,[f] Cristina Tubaro,[a] Marco Baron*[a] and Martina Dell'Angela*[c]

Stable fluorine and chlorine decorated Thiele-like diradicaloids were synthesized and studied in solution and in thin films. Femtosecond transient absorption measurements showed, for both molecules, charge-separated states in solution, but only short-lived singlets in thin films, with no evidence of twisted or charge-separated intermediates. This suppression of excited-state dynamics reflects the strong intermolecular interactions in the solid state and limits their singlet fission potential, highlighting key design challenges for implementing diradicaloids in solid-state optoelectronic and photovoltaic devices.

Stable luminescent diradicals exhibit remarkable optical, electronic, and magnetic properties that are fundamentally different from those of closed-shell luminescent molecules and monoradicals, owing to their unique electronic structures.[1–8] While these exceptional characteristics offer significant potential for diverse applications—including organic light-emitting diodes (OLEDs), magnetoluminescence, thermally activated emission, spin-optical interfaces, bioimaging, and phototherapy—their full potential remains largely unexplored and underutilized in practical implementations.[9–16] Particularly attractive is their potential in singlet fission (SF).[17,18] Yet, isolating molecules that present both two unpaired electrons capable of exhibiting SF and stability at room temperature and in air remains a considerable challenge.[11] These properties are essential for the photovoltaic application of such species, as exploiting SF can potentially surpass the Shockley–Queisser limit in photovoltaic devices.[19,20]

Recent work from Blasi's[21] and Perepichka's[22] groups have demonstrated the synthesis of Thiele-like diradicaloids, decorated with chlorine (**TTH**) or fluorine (**TFH**) atoms (Fig. 1), as stable diradicaloid scaffolds with suitable diradical character for SF. The halogens not only provide the desired stability, but they impart the correct diradical character (y_0) to get efficient SF process.[23] Moreover, theoretical analysis by Messelberger *et al.*[24] shows that the singlet and triplet energies of Thiele diradicaloids closely resemble those of tetracene, a known SF material, suggesting that the energetic landscape of these systems could support singlet fission. Quantum-chemical calculations revealed that their photophysics involves charge-resonance mixing and conformational twisting of an exocyclic bond, yielding zwitterionic charge-separated states.[25] However, all experimental investigations have been limited to solution. Motivated by potential solid-state applications, we synthesized both diradicaloids (**TTH** and **TFH**) and studied their behaviour in thin films, where molecular packing and strong intermolecular interactions were expected to restrict conformational twisting. A deeper understanding of how molecular conformation governs the excited-state dynamics

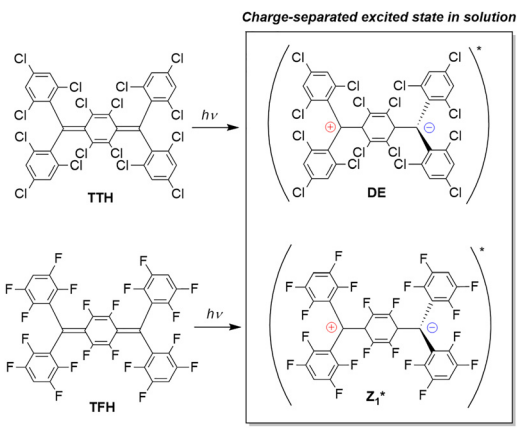

Fig. 1 **TTH** and **TFH** Thiele-like diradicaloids studied in this work and their charge separated excited state in solution. DE = doubly excited state, Z_1^* = zwitterionic excited state.

[a] *Dipartimento di Scienze Chimiche, Università degli Studi di Padova, via F. Marzolo 1, Padova, 35131, Italy. E-mail: marco.baron@unipd.it*
[b] *Dipartimento di Fisica, Università di Trieste, Via Valerio 2, Trieste, 34127, Italy*
[c] *CNR—Istituto Officina dei Materiali (IOM), S.S. 14 km 163.5, Trieste, 34149, Italy. E-mail: dellangela@iom.cnr.it*
[d] *Dipartimento di Scienze Chimiche e Farmaceutiche, Università di Trieste, Via L. Giorgieri 1, Trieste, 34127, Italy*
[e] *Elettra-Sincrotrone Trieste S.C.p.A., Strada Statale 14-km 163.5 in AREA Science Park, Basovizza, Trieste, 34149, Italy*
[f] *Dipartimento di Scienze Chimiche, della Vita e della Sostenibilità Ambientale Università di Parma Parco Area delle Scienze 17/a, I-43124, Parma, Italy*

of Thiele-like radicals could reveal important insights for molecular design and enable the development of solid-state devices based on singlet fission. Here we report the first comparative study of **TTH** and **TFH** in thin films. Transient absorption spectroscopy confirms that while charge-separated states form in solution, in thin films only short-lived singlets are observed. This behaviour is fully consistent with expectations based on the condensed-phase packing: strong intermolecular interactions prevent the rotation required to reach the twisted charge-separated configurations. These results demonstrate that the solid-state environment imposes intrinsic limits on singlet fission in these systems and provide guidance for the rational design of diradicaloids in solid-state optoelectronic and photovoltaic devices.

We started with the synthesis of the **TTH** and **TFH** precursors, named **[TTH]H$_2$** and **[TFH]H$_2$**. As reported in the literature,[21] **[TTH]H$_2$** was isolated exploiting a Friedel–Crafts reaction between 1,2,4,5-tetrachloro-3,6-bis(dichloromethyl)benzene and 1,3,5-trichlorobenzene. The same reaction was employed to isolate **[TFH]H$_2$**, using the corresponding fluorine-substituted reagents.[22] Crystals suitable for single-crystal X-ray diffraction (SCXRD) were successfully grown by slow evaporation of a dichloromethane solution of **[TTH]H$_2$**. As expected, **[TTH]H$_2$** structure (Fig. S15) presents only two sp^3 hybridized carbons (C_{sp3}), as confirmed by the bond distance C_{sp3}–C_{ring} (1.504(12) Å), while the remaining carbons are sp^2 hybridized (C_{sp2}), belonging to exocyclic $C_6Cl_3H_2$ or central C_6Cl_4 aromatic rings, presenting therefore classical bond distances C_{sp2}–C_{sp2} in the range 1.414(12)–1.387(11) Å. As already reported by Blasi *et al.*,[21] the synthesis of **TTH** consists in a first deprotonation of **[TTH]H$_2$**, using [N^{n}Bu$_4$](OH) as a base, obtaining the corresponding di-carbanion [N^{n}Bu$_4$]$_2$[TTH], followed by a second step of oxidation, using an excess of *p*-chloranil, affording **TTH** with low purity. Indeed, using UV-Vis spectroscopy, it was possible to detect the presence of mono-radical as impurity. A subsequent photobleaching step allowed the isolation of highly pure **TTH**, whose successful synthesis and purity were confirmed (see SI). The synthesis of **TFH** is analogous but starting from **[TFH]H$_2$** and using atmospheric air as oxidant. The two diradicaloids synthesized in this work are illustrated in Fig. 1.

Thin films of **TTH** and **TFH** of several molecular layers were deposited onto indium tin oxide (ITO)-coated glass substrates *via* thermal evaporation under ultra-high vacuum conditions (UHV) through a Knudsen type evaporator. The **TTH** and **TFH** powders were loaded in quartz crucibles and heated in UHV at 220 °C and 180 °C respectively. The film quality was assessed using X-ray photoelectron spectroscopy (XPS) measurements conducted at the ANCHOR-SUNDYN endstation at the ALOISA beamline of Elettra synchrotron (Italy).[26] Film thickness was measured to be about 65 nm for both films (see SI). The **TTH** and **TFH** solutions were prepared by dissolving the powders in toluene or acetone to obtain saturated solutions. Fig. 2 shows the C 1s, F 1s, and Cl 2p core level X-ray photoemission (XPS) spectra for both samples. **TTH** was characterized by using synchrotron light at 400 eV photon energy (0.1 eV energy resolution), whereas **TFH** was measured with an Al K-alpha X-ray source (1486.7 eV, 0.3 eV energy resolution). The energy scale on both spectra was referenced by setting the C–C component at 284.8 eV, to account

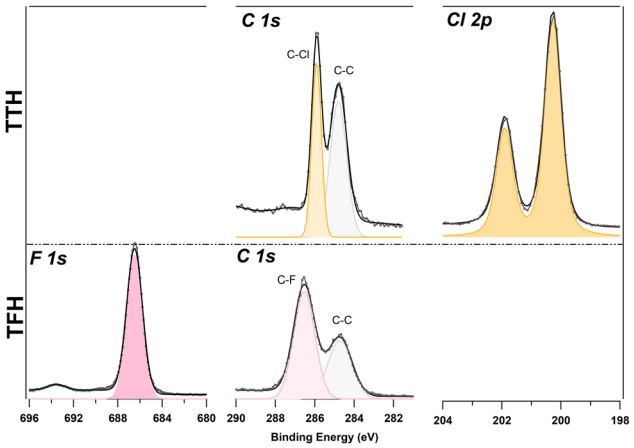

Fig. 2 XPS spectra of F 1s, C 1s and Cl 2p measured on both **TTH** (top panel) and **TFH** (bottom panel) films with 400 eV photon energy and an Al K-alpha X-ray source (1486.7 eV) respectively. Two components have been observed in the C1s core level, attributed to the different chemical states of the carbon atoms in the molecule.

for sample charging.[27] Through spectral deconvolution by using Gaussian peak fitting, we identify in C 1s chemically inequivalent C–F and C–Cl components at 286.6 eV and 285.9 eV, respectively. **TFH** films were stable under X-ray illumination and the intensity ratio $I_{C–C}/I_{C–F}$ was 0.62, matching its stoichiometric ratio of 0.6. **TTH** films instead exhibited rapid modification upon X-ray exposure (with both synchrotron light and the X-ray source), leading to a strong broadening of the C 1s component assigned to C–Cl and the emergence of an additional Cl component (Fig. S19). The intensity ratio $I_{C–C}/I_{C–Cl}$ measured in the first minutes of irradiation is 1.3, also consistent with the expected stoichiometric ratio of 1. These findings confirm that both molecules remained intact during evaporation. Cl 2p and F 1s signals were consistent with reported values for organic carbon-containing compounds.[28–31]

In order to determine whether the thin films exhibited the charge-separated state similar to the one detected in solution,[21,22] we conducted femtosecond transient absorption spectroscopy (fs-TAS) measurements on the 65 nm films on ITO. The experiments were carried out at the T-ReX laboratory (FERMI at Elettra, Trieste) using a Ti:sapphire femtosecond laser source (Coherent Legend Elite DUO He+ USP), producing ≈35 fs light pulses at a repetition rate of 1 kHz, with a central wavelength of 795 nm and a spectral bandwidth of 30 nm. A large fraction of the laser output seeds an optical parametric amplifier (OPA), which generates the wavelength-tunable pump pulse. A broadband supercontinuum probe beam was generated using a small fraction of the laser output, focused in a sapphire window for **TTH** and in a CaF_2 window for **TFH**, covering a spectral range exceeding the 500–1000 nm interval.

Fig. 3(a) and (b) show the 2D fs-TAS measured for **TTH** and **TFH** solutions in acetone, respectively. The corresponding thin film data are reported in Fig. 3(c) and (d). Excitation wavelengths were chosen to match the absorption of the two compounds: 515 nm for **TTH** and 420 nm for **TFH** (see SI Fig. S4 and S5). The two solution's spectra are very similar to each other, as are the two

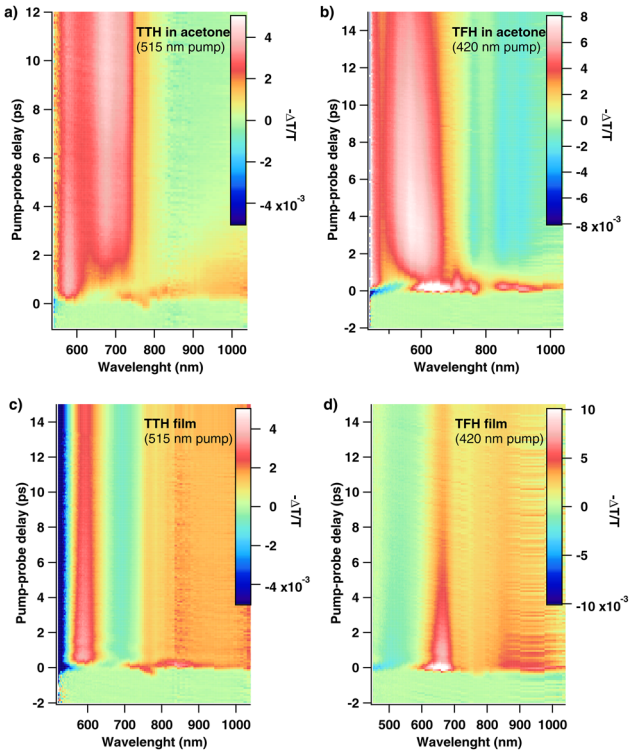

Fig. 3 fs-TAS measurements of **TTH** (a) and **TFH** (b) in acetone and of **TTH** (c) and **TFH** (d) thin films. **TTH** is pumped at 515 nm and **TFH** at 420 nm.

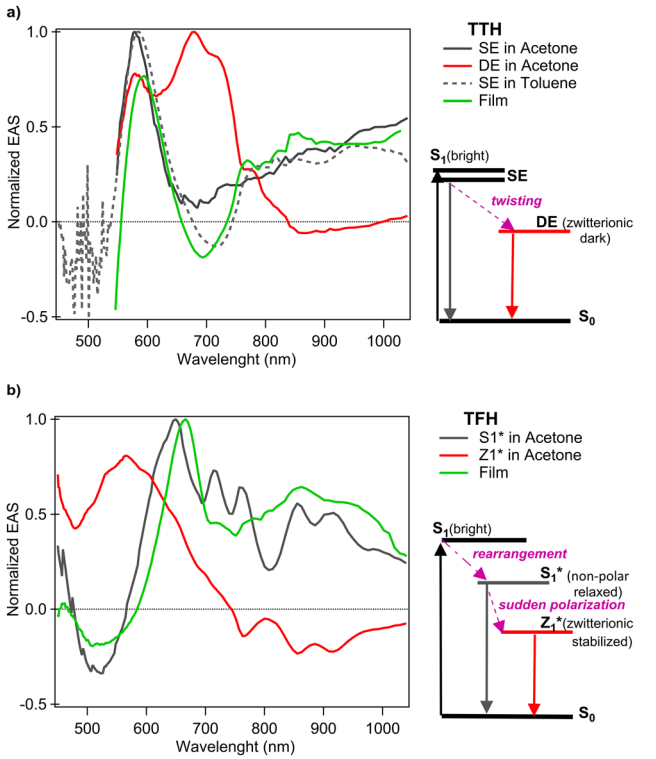

Fig. 4 Normalized evolution associated spectra (EAS) of **TTH** (a) and **TFH** (b) recorded in solution and in thin films. For each molecule, the corresponding Jablonski diagrams describing the solution-state dynamics are shown on the right with the state labelling as reported in the original articles in the literature.[21,22]

film's spectra, but the latter differ significantly from the in-solution spectra. To interpret the spectral dynamics in acetone, we compared our data with the previously reported photophysical models of these molecules.[21,22] A global fit with sequential analysis was performed using the Glotaran software package.[32] The resulting normalized evolution associated spectra (EAS) for **TTH** and **TFH** solutions are shown in Fig. 4(a) and (b) respectively, capturing dynamics beyond 500 fs. For **TTH**, additional measurements were performed in apolar toluene to benchmark against earlier studies.[21] The Jablonski diagrams for both molecules are shown with the state labelling as reported in literature.[21,22] In the semi-polar acetone solution, our analysis confirms that both **TTH** and **TFH** populate zwitterionic charge-separated states. For **TTH** (Fig. 4(a)), the singlet excited state (SE) is observed in both apolar (toluene, dashed curve) and semi-polar (acetone, dark grey curve) environments, consistent with ref. 21. The spectra for the SE state are very similar for the different solvents, showing excited state absorption (ESA) at approximately 580 nm, ground state bleaching (GSB) at 510 nm (overlapping with the pump), and stimulated emission at 700 nm (in toluene). In acetone, SE decays mono-exponentially with a lifetime of τ = 1.7 ps (as reported in the SI Fig. S21). In semi-polar media, **TTH** further accesses the doubly excited (DE) rotated state (Fig. 4(a), red line), which introduces additional ESA around 700 nm and persists within our detection window, reflecting its strong solvent dependence. The doubly excited state (DE) of **TTH** is strongly solvent-polarity dependent, being stabilized and populated in semi-polar media (*e.g.*, acetone) due to its charge-transfer character, but suppressed in non-polar solvents (*e.g.*, toluene), where only the SE state is observed. **TFH** (Fig. 4(b)) displays a similar behaviour. Upon photoexcitation, **TFH** relaxes from the Franck–Condon region to a nonpolar metastable minimum (S1*, relaxed singlet excited state), before twisting into the emissive zwitterionic state (Z1*).[22] Using a two-component global fit for **TFH** in acetone, we identified the S1* and Z1* states, consistent with observations by C. Liu *et al.*, reported as grey and red traces in Fig. 4(b). **TFH** rapidly forms an ESA around 700 nm, which decays monoexponentially with τ = 1.1 ps, corresponding to the S1* state (Fig. S21). Z1* has a lifetime longer than the detection range of our fs-TAS setup.

These findings are consistent with prior reports[21,22] and confirm solvent-dependent stabilization of twisted charge-separated states. A striking difference arises in the thin films. In both **TTH** and **TFH**, the global fit (Fig. 4(a) and (b), green lines) yields only a single spectral component resembling the SE state of **TTH** and the S1* state of **TFH** in solution. Crucially, no signatures of the twisted states (DE in **TTH**, Z1* in **TFH**) are observed. This absence indicates that in the solid state the conformational twisting needed to reach the emissive zwitterionic configurations does not occur or is suppressed to the point of being spectroscopically inaccessible. Since the rotated states have been linked to triplet formation pathways, their absence in the film points to a fundamentally different excited-state relaxation landscape compared to solution. Thus, while halogenation stabilizes diradicaloids and permits charge

separation in solution, these pathways are effectively quenched in the condensed phase. The suppression of charge-separated intermediates in thin films underscores the critical role of conformational freedom in diradicaloid photophysics. To further probe the origin of this behavior, we performed femtosecond transient absorption measurements on **TFH** embedded in an inert organic matrix (see SI, Fig. S22). PVA films can rigidly trap chromophore molecules, suppressing large-scale translational diffusion or reorientation, reducing phenomena such as aggregation.[33–35] Despite the reduced molecular density and minimal intermolecular interactions in the matrix, the transient absorption signal is spectrally and kinetically identical to that of the pure thin film. This finding confirms that conformational restriction, rather than interchromophoric coupling or polarity effects, is the dominant factor driving the rapid excited-state deactivation in the solid state. Strategies to restore solution-like behavior—such as embedding molecules in tailored host matrices, co-crystallization, or designing side groups that preserve flexibility—may enable solid-state singlet fission in future systems.

In conclusion, we synthesized and studied halogenated Thiele-like diradicaloids both in solution and as thin films. In solution, both **TTH** and **TFH** populate zwitterionic charge-separated states through conformational twisting, in agreement with previous reports. However, in thin films we found only short-lived singlets, with no spectroscopic signatures of the twisted or charge-separated intermediates. This result confirms our expectation that strong intermolecular interactions in the solid state restrict the molecular flexibility required to reach rotated configurations. The suppression of these key intermediates in the condensed phase imposes a fundamental limitation on singlet fission in these systems. Our findings thus provide clear guidance for the design of diradicaloids: strategies that preserve conformational freedom (such as host–guest embedding, co-crystallization, or side-group engineering) will be essential for enabling solid-state singlet fission and advancing their application in optoelectronic and photovoltaic devices.

M. Be., C. G., C. T. and L. S. performed the experimental work, contributed to data curation, and assisted in revising the manuscript. L. C., R. C., P. O., and A. C. contributed to the investigation. F. C., M. Ba., and M. D. A. conceived and designed the project, supervised the research, acquired funding, and wrote the original manuscript. All authors have given approval to the final version of the manuscript.

M. D. A., F. C., M. Be., C. T., M. Ba. gratefully acknowledge the financial support from under the National Recovery and Resilience Plan (NRRP), Mission 4, Component 2, Investment 1.1, Call for tender No. 104 published on 2.2.2022 by the Italian MUR, funded by the European Union – NextGenerationEU – Project MEGS – CUP B53D23003930006.

Conflicts of interest

There are no conflicts to declare.

Data availability

Data for this article, including XPS and fs-TAS raw data, are available at https://doi.org/10.34965/I60482.

Supplementary information (SI) is available. See DOI: https://doi.org/10.1039/d5cc05557a.

References

1 G. E. Rudebusch, J. L. Zafra, K. Jorner, K. Fukuda, J. L. Marshall, I. Arrechea-Marcos, G. L. Espejo, R. Ponce Ortiz, C. J. Gómez-García, L. N. Zakharov, M. Nakano, H. Ottosson, J. Casado and M. M. Haley, *Nat. Chem.*, 2016, **8**, 753–759.
2 C. Zong, S. Yang, Y. Sun, L. Zhang, J. Hu, W. Hu, R. Li and Z. Sun, *Chem. Sci.*, 2022, **13**, 11442–11447.
3 S. Lukman, J. M. Richter, L. Yang, P. Hu, J. Wu, N. C. Greenham and A. J. Musser, *J. Am. Chem. Soc.*, 2017, **139**, 18376–18385.
4 M. Ballester, J. Riera-Figueras, J. Castaner, C. Badfa and J. M. Monso, *J. Am. Chem. Soc.*, 1971, **93**, 2215–2225.
5 M. Ballester, I. Pascual, C. Carreras and J. Vidal-Gancedo, *J. Am. Chem. Soc.*, 1994, **116**, 4205–4210.
6 M. Ballester, J. Castaner, J. Riera and I. Pascual, *J. Am. Chem. Soc.*, 1984, **106**, 3365–3366.
7 O. Varnavski, N. Abeyasinghe, J. Aragó, J. J. Serrano-Pérez, E. Ortí, J. T. López Navarrete, K. Takimiya, D. Casanova, J. Casado and T. Goodson, *J. Phys. Chem. Lett.*, 2015, **6**, 1375–1384.
8 J. Castaner and J. Riera, *J. Org. Chem.*, 1991, **56**, 5445–5448.
9 X. Chang, M. E. Arnold, R. Blinder, J. Zolg, J. Wischnat, J. van Slageren, F. Jelezko, A. J. C. Kuehne and M. von Delius, *Angew. Chem., Int. Ed.*, 2024, **63**, e202404853.
10 A. Abdurahman, J. Wang, Y. Zhao, P. Li, L. Shen and Q. Peng, *Angew. Chem., Int. Ed.*, 2023, **62**, e202300772.
11 Y. Zhu, Z. Zhu, S. Wang, Q. Peng and A. Abdurahman, *Angew. Chem., Int. Ed.*, 2025, **64**, e202423470.
12 S. Mori, S. Moles Quintero, N. Tabaka, R. Kishi, R. González Núñez, A. Harbuzaru, R. Ponce Ortiz, J. Marín-Beloqui, S. Suzuki, C. Kitamura, C. J. Gómez-García, Y. Dai, F. Negri, M. Nakano, S. Kato and J. Casado, *Angew. Chem., Int. Ed.*, 2022, **61**, e202206680.
13 H. Koike, M. Chikamatsu, R. Azumi, J. Tsutsumi, K. Ogawa, W. Yamane, T. Nishiuchi, T. Kubo, T. Hasegawa and K. Kanai, *Adv. Funct. Mater.*, 2016, **26**, 277–283.
14 T. Kubo, A. Shimizu, M. Sakamoto, M. Uruichi, K. Yakushi, M. Nakano, D. Shiomi, K. Sato, T. Takui, Y. Morita and K. Nakasuji, *Angew. Chem., Int. Ed.*, 2005, **44**, 6564–6568.
15 K. Yang, X. Zhang, A. Harbuzaru, L. Wang, Y. Wang, C. Koh, H. Guo, Y. Shi, J. Chen, H. Sun, K. Feng, M. C. Ruiz Delgado, H. Y. Woo, R. P. Ortiz and X. Guo, *J. Am. Chem. Soc.*, 2020, **142**, 4329–4340.
16 A. Abdurahman, L. Shen, J. Wang, M. Niu, P. Li, Q. Peng, J. Wang and G. Lu, *Light: Sci. Appl.*, 2023, **12**, 272.
17 S. Lukman, J. M. Richter, L. Yang, P. Hu, J. Wu, N. C. Greenham and A. J. Musser, *J. Am. Chem. Soc.*, 2017, **139**, 18376–18385.
18 J. Messelberger, A. Grünwald, P. Pinter, M. M. Hansmann and D. Munz, *Chem. Sci.*, 2018, **9**, 6107–6117.
19 W. Shockley and H. J. Queisser, *J. Appl. Phys.*, 1961, **32**, 510–519.
20 C. A. Nelson, N. R. Monahan and X.-Y. Zhu, *Energy Environ. Sci.*, 2013, **6**, 3508.
21 A. Punzi, Y. Dai, C. N. Dibenedetto, E. Mesto, E. Schingaro, T. Ullrich, M. Striccoli, D. M. Guldi, F. Negri, G. M. Farinola and D. Blasi, *J. Am. Chem. Soc.*, 2023, **145**, 20229–20241.
22 C.-H. Liu, Z. He, C. Ruchlin, Y. Che, K. Somers and D. F. Perepichka, *J. Am. Chem. Soc.*, 2023, **145**, 15702–15707.
23 Q. Sun, J.-L. Brédas and H. Li, *J. Chem. Theory Comput.*, 2025, **21**, 1194–1202.
24 J. Messelberger, A. Grünwald, P. Pinter, M. M. Hansmann and D. Munz, *Chem. Sci.*, 2018, **9**, 6107–6117.
25 D. Mesto, M. Orza, B. Bardi, A. Punzi, I. Ratera, J. Veciana, G. Farinola, A. Painelli, F. Terenziani, D. Blasi and F. Negri, *Chem. – Eur. J.*, 2025, **31**, e202500749.
26 R. Costantini, M. Stredansky, D. Cvetko, G. Kladnik, A. Verdini, P. Sigalotti, F. Cilento, F. Salvador, A. De Luisa, D. Benedetti, L. Floreano, A. Morgante, A. Cossaro and M. Dell'Angela, *J. Electron Spectrosc. Relat. Phenom.*, 2018, **229**, 7–12.

27 G. Greczynski and L. Hultman, *Appl. Surf. Sci.*, 2022, **606**, 154855.
28 E. Barrena, R. Palacios-Rivera, A. Babuji, L. Schio, M. Tormen, L. Floreano and C. Ocal, *Phys. Chem. Chem. Phys.*, 2022, **24**, 2349–2356.
29 G. Galeotti, M. Di Giovannantonio, J. Lipton-Duffin, M. Ebrahimi, S. Tebi, A. Verdini, L. Floreano, Y. Fagot-Revurat, D. F. Perepichka, F. Rosei and G. Contini, *Faraday Discuss.*, 2017, **204**, 453–469.
30 J. Dai, W. Zhao, L. Xing, J. Shang, H. Ju, X. Zhou, J. Liu, Q. Chen, Y. Wang, J. Zhu and K. Wu, *ChemPhysChem*, 2019, **20**, 2367–2375.
31 S. L. Wong, H. Huang, Y. L. Huang, Y. Z. Wang, X. Y. Gao, T. Suzuki, W. Chen and A. T. S. Wee, *J. Phys. Chem. C*, 2010, **114**, 9356–9361.
32 J. J. Snellenburg, S. P. Laptenok, R. Seger, K. M. Mullen and I. H. M. van Stokkum, *J. Stat. Softw.*, 2012, **49**, 1–22.
33 Q. Liu, F. Wackenhut, O. Hauler, M. Scholz, S. Zur Oven-Krockhaus, R. Ritz, P. M. Adam, M. Brecht and A. J. Meixner, *J. Phys. Chem. A*, 2020, **124**, 2497–2504.
34 R. Chib, S. Raut, S. Shah, B. Grobelna, I. Akopova, R. Rich, T. J. Sørensen, B. W. Laursen, H. Grajek, Z. Gryczynski and I. Gryczynski, *Dyes Pigm.*, 2015, **117**, 16–23.
35 J. N. Clifford, T. D. M. Bell, P. Tinnefeld, M. Heilemann, S. M. Melnikov, J. I. Hotta, M. Sliwa, P. Dedecker, M. Sauer, J. Hofkens and E. K. L. Yeow, *J. Phys. Chem. B*, 2007, **111**, 6987–6991.